Derivation and Implementation of the Gradient of the R^{-7} Dispersion Interaction in the Effective Fragment Potential Method

Emilie B Guidez, Peng Xu, and Mark S. Gordon*

Department of Chemistry, Iowa State University, Ames, Iowa 50011, United States

ⓢ Supporting Information

ABSTRACT: The dispersion interaction energy may be expressed as a sum over R^{-n} terms, with $n \geq 6$. Most implementations of the dispersion interaction in model potentials are terminated at $n = 6$. Those implementations that do include higher order contributions commonly only include even power terms, despite the fact that odd power terms can be important. Because the effective fragment potential (EFP) method contains no empirically fitted parameters, the EFP method provides a useful vehicle for examining the importance of the leading R^{-7} odd power term in the dispersion expansion. To fully evaluate the importance of the R^{-7} contribution to the dispersion energy, it is important to have analytic energy first derivatives for all terms. In the present work, the gradients of the term $E_7 \sim R^{-7}$ are derived analytically, implemented in the GAMESS software package, and evaluated relative to other terms in the dispersion expansion and relative to the total EFP interaction energy. Periodic boundary conditions in the minimum image convention are also implemented. A more accurate dispersion energy contribution can now be obtained during molecular dynamics simulations.
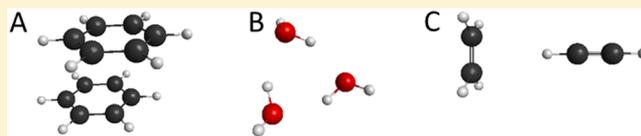
INTRODUCTION

Dispersion derives from the intermolecular forces that arise from the interaction of induced multipoles between atoms and molecules.[1] The dispersion interaction between two molecular species can be expressed as[2]

$$E_{disp} = E_6 + E_7 + E_8 \ldots$$
$$= C_6/R^6 + C_7/R^7 + C_8/R^8 + \ldots \quad (1)$$

The E_6 term arises from the interaction between induced dipoles. The origin of the E_7 term is the interaction between induced dipoles and induced quadrupoles. The E_8 term comes from induced quadrupole-induced quadrupole interactions and from induced dipole-induced octopole interactions, and so on. E_6 is the leading term and a wide variety of methods have been developed to calculate it, with various approximations, including the use of fitted parameters. For instance, the dispersion energy is often included in an *ad hoc* manner in DFT calculations using parametrized atomic pairwise interactions.[3−6] Parameter-free methods have been developed by Tkatchenko[7−9] and Becke.[10] In addition, several methods have been developed to calculate the contribution of the dispersion energy to the free energy of solvation.[11−16] Odd order terms in eq 1 average to zero in freely rotating systems and are often neglected. Higher order contributions are often neglected since it is usually assumed that they are much smaller than the leading term. However, this is not necessarily the case.[17]

The E_7 contribution to the dispersion energy is highly dependent on the orientation of the interacting molecules. It is often neglected since it averages to zero in freely rotating systems (assuming all orientations have equal weights). However, E_7 values can be non-negligible at a given orientation.[18] For instance, E_7 represents over 50% of the E_6 value for the water and ammonia dimers at their equilibrium geometry.[18] Another important point is that contrary to E_6 which is always negative, E_7 can be either positive or negative depending on the relative orientation of the interacting molecules.[18] As a result, E_7 cannot be estimated from E_6. It is reasonable to expect that systems in which the rotational motion is hindered in some way (e.g., very viscous systems) or in which the rotational motions are inherently slow (e.g., large molecules of interest in biology or materials science) may have a significant E_7 contribution to the dispersion energy. It is important to analyze and understand the interactions between molecules in such systems in order to accurately model their properties.

One method that has been used successfully to describe solvents quantum mechanically is the effective fragment potential (EFP) method.[19,20] With this method, rigid solvent molecules are modeled with a potential and the interaction between them is decomposed into five terms: Coulomb, polarization, exchange repulsion, charge transfer and dispersion:

$$E = E_{coul} + E_{pol} + E_{exrep} + E_{ct} + E_{disp} \quad (2)$$

An advantage of the EFP method is that all of the terms, including dispersion, are derived from first-principles and contain no empirically fitted parameters. Consequently, interpretations of the relative importance of various terms in the interaction energy do not rely on such parameters. All energy terms and their gradients have been derived and implemented in the GAMESS[21,22] software package.[17,23−26]

The EFP method is available in other electronic structure packages as well.[27,28] For the dispersion term, the E_6 contribution to the energy and gradients have been derived and implemented.[17] The E_8 term is currently approximated as $^1/_3 E_6$. The E_7 energy term was implemented by Xu et al.[18] It should be emphasized that the dispersion energy in the EFP method (and many of the methods mentioned above) only considers pairwise interactions. It is worth mentioning that many-body effects may be important[29,30] and methods to include them are under active development.[31−34]

In this paper, the E_7 gradient is derived and tested. In the methods section, the expression for the E_6 energy term and gradient are summarized,[17] and the gradient of the E_7 energy term is derived. The computational details are given next, followed by a comparison between numerical and analytic gradients for a few test cases. A geometry optimization and a molecular dynamics simulation using the minimum image convention are also performed.

■ METHODS

Expression for the EFP Dispersion Energies. Localized molecular orbitals (LMOs) play a central role in the formulation of the dispersion, exchange-repulsion, charge transfer and polarization terms in the EFP method. LMOs are mathematically equivalent to the canonical molecular orbitals (CMOs) but provide a more intuitive description of chemical bonding. In addition, the EFP energy contributions are expressed as truncated series which converge faster and yield more accurate results when using the LMO formulation.[18,35,36] For the dispersion interaction, it is the LMO dynamic (frequency dependent) polarizabilities that are used in the formulation. The total dispersion energy between EFP fragments can be written in a form similar to eq 1 where the dispersion energy between two fragments is summed over all LMO pairs, one on each fragment. Within the EFP method, the $E_{6,0}$ dispersion term (the 0 subscript indicates that no damping is included) between two molecules A and B can be expressed as[17]

$$E_{6,0}^{AB} = -\frac{\hbar}{2\pi} \sum_{k \in A} \sum_{j \in B} \sum_{\alpha\beta\gamma\delta}^{x,y,z} T_{\alpha\beta}^{kj} T_{\gamma\delta}^{kj} \int_0^\infty \alpha_{\alpha\gamma}^k(i\omega) \alpha_{\beta\delta}^j(i\omega) \, d\omega \tag{3}$$

Indices A and B label the EFP fragments or molecules, k and j label the localized molecular orbitals[37] of fragments A and B respectively. The Greek letters α, β, γ, and δ label the x, y, or z axis. T corresponds to the second order electrostatic tensor, which can be expressed as (in atomic units):

$$T_{\alpha\beta}^{kj} = \nabla_\alpha \nabla_\beta \frac{1}{R_{kj}} = \frac{3R_\alpha R_\beta - R_{kj}^2 \delta_{\alpha\beta}}{R_{kj}^5} \tag{4}$$

R_{kj} is the distance between the LMO centroids k and j. In this expression, R_α and R_β represent the x, y or z component of R_{kj}. For instance, $R_x = x_k - x_j$. $\alpha^l(i\omega)$ represents the dynamic dipole−dipole polarizability tensor in the imaginary frequency regime for LMO l. It is obtained by performing a transformation of the canonical molecular orbitals (CMOs) in the expression of the molecular dynamic dipole−dipole polarizability to LMOs. The molecular dynamic dipole−dipole polarizabiliy is obtained by solving the time-dependent Hartree−Fock equations.[17,38] Eq 3 gives the full anisotropic

E_6 dispersion energy and can be simplified to the isotropic form:[17]

$$E_{6,0}^{AB} = -\frac{3\hbar}{\pi} \sum_{k \in A} \sum_{j \in B} \frac{\int_0^\infty \bar{\alpha}^k(i\omega)\bar{\alpha}^j(i\omega) \, d\omega}{R_{kj}^6}$$

$$= \sum_{k \in A} \sum_{j \in B} \frac{C_6^{kj}}{R_{kj}^6} \tag{5}$$

with $C_6^{kj} = -\frac{3\hbar}{\pi} \sum_{k \in A} \sum_{j \in B} \int_0^\infty \bar{\alpha}^k(i\omega)\bar{\alpha}^j(i\omega) \, d\omega$, where $\bar{\alpha}(i\omega)$ represents the trace of the polarizability tensor. Eq 5 can be integrated using a 12-point Gauss-Legendre quadrature formula to give the following:[17]

$$E_{6,0}^{AB} = -\frac{3\hbar}{\pi} \sum_{k \in A} \sum_{j \in B} \sum_{i=1}^{12} W_i \frac{2\omega_0}{(1 - t_i)^2} \frac{\bar{\alpha}^k(i\omega_i)\bar{\alpha}^k(i\omega_i)}{R_{kj}^6} \tag{6}$$

W_i and t_i are the Gauss−Legendre weighting factor and abscissa, respectively. $E_{6,0}$ must be multiplied by a damping function to avoid poor behavior near $R_{kj} = 0$.[1] The damping function used in the EFP method is based on the intermolecular overlap.[39] For the $E_{6,0}$ term, the damping function is[39]

$$f_6(k, j) = 1 - S_{kj}^2 \sum_{n=0}^6 \frac{(-2 \ln|S_{kj}|)^{n/2}}{n!} \tag{7}$$

In eq 7, S_{kj} is the overlap between the LMOs k and j. Henceforth, the convention for the expression of the dipole−dipole contribution to the dispersion energy is

$$E_6 = f_6 E_{6,0} \tag{8}$$

In eq 8, f_6 is the damping function given in eq 7. A similar convention will be used for the higher order terms in the dispersion expansion, eq 1.

Xu et al. derived the expression for the value of the E_7 interaction energy between two EFP fragments:[18]

$$E_{7,0} = -\frac{\hbar}{3\pi} \sum_{k \in A} \sum_{j \in B} \sum_{\alpha\beta\gamma\sigma\kappa}^{x,y,z} T_{\alpha\beta}^{kj} T_{\gamma\sigma\kappa}^{kj}$$

$$\times \int_0^\infty d\omega \, [\alpha_{\alpha\gamma}^k(i\omega) A_{\beta,\sigma\kappa}^j(i\omega) - \alpha_{\beta\kappa}^j(i\omega) A_{\alpha,\gamma\sigma}^k(i\omega)] \tag{9}$$

$T_{\gamma\sigma\kappa}^{kj}$ is the third order electrostatic tensor given by

$$T_{\gamma\sigma\kappa}^{kj} = \nabla_\gamma \nabla_\sigma \nabla_\kappa \frac{1}{R_{kj}}$$

$$= -\frac{15 R_\gamma R_\sigma R_\kappa - 3R_{kj}^2 (R_\gamma \delta_{\sigma\kappa} + R_\sigma \delta_{\gamma\kappa} + R_\kappa \delta_{\gamma\sigma})}{R_{kj}^7} \tag{10}$$

A^l represents the dynamic dipole−quadrupole polarizability expanded at the centroid of LMO l. Briefly, the molecular dipole−quadrupole polarizability at the center of mass is first obtained from the solution of the time-dependent Hartree−Fock equations.[40] Then, the dipole−quadrupole polarizability contribution from each LMO is obtained by transformation of the canonical orbitals to LMOs followed by a shift to the LMO centroid.[18] This shifting procedure is necessary since unlike the dipole−dipole dynamic polarizabilities, dynamic dipole−quadrupole polarizabilities are origin-dependent.[18] All other terms

in eq 9 are defined in the same way as the terms in eq 3. The integral in eq 9 can be evaluated using the 12-point Gauss–Legendre quadrature formula as in eq 6:

$$E_{7,0} = -\frac{\hbar}{3\pi} \sum_{k\in A} \sum_{j\in B} \sum_{\alpha\beta\gamma\sigma\kappa}^{x,y,z} \sum_{i=1}^{12} W_i \frac{2\omega_0}{(1-t_i)^2} T_{\alpha\beta}^{kj} T_{\gamma\sigma\kappa}^{kj} [\alpha_{\alpha\gamma}^k(i\omega_i) A_{\beta,\sigma\kappa}^j(i\omega_i)$$
$$- \alpha_{\beta\kappa}^j(i\omega_i) A_{\alpha,\gamma\sigma}^k(i\omega_i)] \quad (11)$$

The multiplicative damping function f_7 for the E_7 term is derived similarly to f_6:

$$f_7(k,j) = 1 - S_{kj}^2 \sum_{n=0}^{7} \frac{(-2 \ln|S_{kj}|)^{n/2}}{n!} \quad (12)$$

Note that E_7 in eq 9 is anisotropic; the isotropic approximation will result in a zero E_7 dispersion energy.

Gradients of the E_6 and E_7 Terms. The derivation of the E_6 gradient is briefly mentioned, followed by a more detailed derivation of the E_7 gradient. First the gradient expressions with respect to an arbitrary variable are presented. EFP fragments are rigid, so only the translational and rotational degrees of freedom need to be considered. A detailed derivation of both translational and rotational gradients is presented. Lastly, for the conservation of energy during molecular dynamics (MD) simulations, switching functions and their derivatives are implemented.

The general expression for the E_6 gradient is

$$\frac{\partial E_6}{\partial q_A} = \frac{\partial\left[\sum_{k\in A}\sum_{j\in B}\frac{C_6(j,k)f_6(j,k)}{R_{kj}^6}\right]}{\partial q_A}$$
$$= \sum_{k\in A}\sum_{j\in B}\left[\left[\frac{\partial C_6(j,k)}{\partial q_A}f_6(j,k) + C_6(j,k)\frac{\partial f_6(j,k)}{\partial q_A}\right]R_{jk}^{-6}\right.$$
$$\left. - 6[C_6(j,k)f_6(j,k)]R_{kj}^{-7}\frac{\partial R}{\partial q_A}\right]$$
$$= \sum_{k\in A}\sum_{j\in B}\left[C_6(j,k)\frac{\partial f_6(j,k)}{\partial q_A}\right]R_{kj}^{-6} - 6[C_6(j,k)f_6(j,k)]R_{kj}^{-7}\frac{\partial R}{\partial q_A} \quad (13)$$

$\frac{\partial C_6(j,k)}{\partial q_A} = 0$ since C_6 is a constant. The derivative of the damping function can be written as

$$\frac{\partial f_6(j,k)}{\partial q_A} = -S_{kj}\left(\frac{\partial S_{kj}}{\partial q_A}\right)\left(1 + \frac{3}{2}\sqrt{-2\ln|S_{kj}|} - \frac{1}{\sqrt{-2\ln|S_{kj}|}}\right.$$
$$+ \frac{5}{6}(-2\ln|S_{kj}|) + \frac{7}{24}(-2\ln|S_{kj}|)^{3/2}$$
$$+ \frac{9}{120}(-2\ln|S_{kj}|)^2 + \frac{1}{60}(-2\ln|S_{kj}|)^{5/2}$$
$$\left. + \frac{1}{360}(-2\ln|S_{kj}|)^3\right) \quad (14)$$

The general expression of the gradient of the E_7 term is given by

$$\frac{\partial E_7}{\partial q_A} = \frac{\partial f_7}{\partial q_A}E_{7,0} + f_7\frac{\partial E_{7,0}}{\partial q_A} \quad (15)$$

The derivative of the undamped energy $E_{7,0}$ is given by

$$\frac{\partial E_{7,0}}{\partial q_A} = -\frac{\hbar}{3\pi}\sum_{k\in A}\sum_{j\in B}\sum_{\alpha\beta\gamma\sigma\kappa}^{x,y,z}\sum_{i=1}^{12}\frac{\partial}{\partial q_A}\left(T_{\alpha\beta}^{kj}T_{\gamma\sigma\kappa}^{kj}W(i)\frac{2\omega_0}{(1-t_i)^2}\right.$$
$$\times [\alpha_{\alpha\gamma}^k(i\omega_i)A_{\beta,\sigma\kappa}^j(i\omega_i) - \alpha_{\beta\kappa}^j(i\omega_i)A_{\alpha,\gamma\sigma}^k(i\omega_i)]\bigg)$$
$$= -\frac{\hbar}{3\pi}\sum_{k\in A}\sum_{j\in B}\sum_{\alpha\beta\gamma\sigma\kappa}^{x,y,z}\sum_{i=1}^{12}\left(W(i)\frac{2\omega_0}{(1-t_i)^2}\right.$$
$$\times [\alpha_{\alpha\gamma}^k(i\omega_i)A_{\beta,\sigma\kappa}^j(i\omega_i) - \alpha_{\beta\kappa}^j(i\omega_i)A_{\alpha,\gamma\sigma}^k(i\omega_i)]\bigg)\frac{\partial(T_{\alpha\beta}^{kj}T_{\gamma\sigma\kappa}^{kj})}{\partial q_A}$$
$$+ T_{\alpha\beta}^{kj}T_{\gamma\sigma\kappa}^{kj}W(i)\frac{2\omega_0}{(1-t_i)^2}\frac{\partial}{\partial q_A}[\alpha_{\alpha\gamma}^k(i\omega_i)A_{\beta,\sigma\kappa}^j(i\omega_i)$$
$$- \alpha_{\beta\kappa}^j(i\omega_i)A_{\alpha,\gamma\sigma}^k(i\omega_i)]$$
$$= -\frac{\hbar}{3\pi}\sum_{k\in A}\sum_{j\in B}\sum_{\alpha\beta\gamma\sigma\kappa\tau\vartheta}^{x,y,z}\sum_{i=1}^{12}\left[\frac{\partial T_{\alpha\beta}^{kj}}{\partial q_A}T_{\gamma\sigma\kappa}^{kj} + T_{\alpha\beta}^{kj}\frac{\partial T_{\gamma\sigma\kappa}^{kj}}{\partial q_A}\right]$$
$$\times W(i)\frac{2\omega_0}{(1-t_i)^2}([\alpha_{\alpha\gamma}^k(i\omega_i)A_{\beta,\sigma\kappa}^j(i\omega_i) - \alpha_{\beta\kappa}^j(i\omega_i)A_{\alpha,\gamma\sigma}^k(i\omega_i)])$$
$$+ T_{\alpha\beta}^{kj}T_{\gamma\sigma\kappa}^{kj}W(i)\frac{2\omega_0}{(1-t_i)^2}$$
$$\times\left[\frac{\partial\alpha_{\alpha\gamma}^k(i\omega_i)}{\partial q_A}A_{\beta,\sigma\kappa}^j(i\omega_i) + \alpha_{\alpha\gamma}^k(i\omega_i)\frac{\partial A_{\beta,\sigma\kappa}^j(i\omega_i)}{\partial q_A}\right.$$
$$\left. - \frac{\partial\alpha_{\beta\kappa}^j(i\omega_i)}{\partial q_A}A_{\alpha,\gamma\sigma}^k(i\omega_i) - \frac{\partial A_{\alpha,\gamma\sigma}^k(i\omega_i)}{\partial q_A}\alpha_{\beta\kappa}^j(i\omega_i)\right] \quad (16)$$

The derivatives of the dynamic dipole–dipole polarizability and dipole–quadrupole polarizability involving LMOs of fragment B with respect to the motion of fragment A are 0:

$$\frac{\partial A_{\beta,\sigma\kappa}^j(i\omega)}{\partial q_A} = 0, \quad \frac{\partial\alpha_{\beta\kappa}^j(i\omega)}{\partial q_A} = 0$$

The derivative of the $f_7(j,k)$ damping function is given by

$$\frac{\partial f_7(j,k)}{\partial q_A} = -S_{kj}\left(\frac{\partial S_{kj}}{\partial q_A}\right)\left(1 + \frac{3}{2}\sqrt{-2\ln|S_{kj}|} - \frac{1}{\sqrt{-2\ln|S_{kj}|}}\right.$$
$$+ \frac{5}{6}(-2\ln|S_{kj}|) + \frac{7}{24}(-2\ln|S_{kj}|)^{3/2}$$
$$+ \frac{9}{120}(-2\ln|S_{kj}|)^2 + \frac{11}{720}(-2\ln|S_{kj}|)^{5/2}$$
$$\left. + \frac{1}{360}(-2\ln|S_{kj}|)^3 + \frac{1}{2520}(-2\ln|S_{kj}|)^{7/2}\right) \quad (17)$$

Since EFP fragments are rigid, the only degrees of freedom that need to be considered for the gradients are translation and rotation which are now described.

Translational Motion of A. In order to calculate the translational derivatives of E_6, the derivatives of the distances R_{kj} and the derivatives of the overlap integrals S_{kj} with respect to the translation of fragment A along the x, y and z axes (denoted x_A, y_A, z_A) are required. The derivative of the distance R_{kj} with respect to the translation of molecule A along the x axis is

$$\frac{\partial R_{kj}}{\partial x_A} = \frac{(x_k - x_j)}{R_{jk}} \quad (18)$$

In eq 18, $x_k - x_j$ is the distance between the x coordinates of the LMO centroids k and j. Since the fragments are rigid, the derivatives of the overlap integrals S_{kj} can be obtained

from the derivatives of the atomic integrals $S_{\mu\nu}$ and they are given by[24]

$$\frac{\partial S_{kj}}{\partial x_A} = \sum_\nu^B c_{\nu j} \sum_\mu^A c_{\mu k} \cdot \sum_a^A \left(\frac{\partial S_{\mu\nu}}{\partial x_a}\right) = \sum_\nu^B c_{\nu j} \sum_\mu^A c_{\mu k} \cdot \sum_a^A \left\langle \frac{\partial \psi_u}{\partial x_a} \Big| \psi_\nu \right\rangle$$

(19)

In eq 19, the subscripts μ and ν label atomic orbitals, while the subscripts k and j label the LMOs. The c coefficients are the LMO coefficients and the functions ψ are the atomic basis functions, and are summed over all of the atoms a in fragment A. The translational derivatives of all of the polarizability tensors are zero since the polarizability does not change upon translation of the fragment. Therefore, only the translational derivatives of the T tensors are needed in order to determine the translational derivative of E_7. The translational derivatives of the nth-order T tensor are related to the $(n + 1)$th-order tensors. The derivative of the second-order T tensor with respect to the translation of fragment A along the x axis is

$$\frac{\partial T_{\alpha\beta}^{kj}}{\partial x_A} = \nabla_x \nabla_\beta \nabla_\alpha \frac{1}{R_{kj}}$$

$$= -\frac{15 R_x R_\alpha R_\beta - 3R_{kj}^2 (R_x \delta_{\alpha\beta} + R_\alpha \delta_{x\beta} + R_\beta \delta_{x\alpha})}{R_{kj}^7}$$

(20)

Similar expressions can be derived for $\frac{\partial T_{\alpha\beta}^{kj}}{\partial y_A}$ and $\frac{\partial T_{\alpha\beta}^{kj}}{\partial z_A}$ (cf., Supporting Information)

Similarly, the derivatives of the third-order T tensor are the fourth-order T tensors:

$$\partial T_{\gamma\sigma\kappa}^{kj} / \partial x_A = \nabla_x \nabla_\gamma \nabla_\sigma \nabla_\kappa 1 / R_{kj}$$

$$= (105 R_x R_\gamma R_\sigma R_\kappa - 15 R_{kj}^2 (R_x R_\gamma \delta_{\sigma\kappa} + R_x R_\sigma \delta_{\gamma\kappa}$$

$$+ R_x R_\kappa \delta_{\gamma\sigma} + R_\gamma R_\sigma \delta_{x\kappa} + R_\gamma R_\kappa \delta_{x\sigma} + R_\sigma R_\kappa \delta_{x\gamma}) / R_{kj}^9$$

$$+ 3 R_{kj}^4 (\delta_{x\gamma} \delta_{\sigma\kappa} + \delta_{x\sigma} \delta_{\gamma\kappa} + \delta_{x\kappa} \delta_{\gamma\sigma}) / R_{kj}^9$$

(21)

The expressions for $\frac{\partial T_{\gamma\sigma\kappa}^{kj}}{\partial y_A}$ and $\frac{\partial T_{\gamma\sigma\kappa}^{kj}}{\partial z_A}$ are given in the Supporting Information.

The forces of B acting on A and the forces of A acting on B must cancel each other:

$$F_x^{A(B)} = -F_x^{B(A)}$$

$$F_y^{A(B)} = -F_y^{B(A)}$$

$$F_z^{A(B)} = -F_z^{B(A)}$$

(22)

Therefore, one only needs to calculate the x, y, and z components of the forces on A induced by B, which are given by

$$F_x^{A(B)} = -\frac{\partial E_{Disp}}{\partial x}$$

$$F_y^{A(B)} = -\frac{\partial E_{Disp}}{\partial y}$$

$$F_z^{A(B)} = -\frac{\partial E_{Disp}}{\partial z}$$

(23)

E_{Disp} is the sum of the E_6, E_7, and E_8 energies described above. Note that the E_8 term is included as $(1/3)$ of E_6.[17]

Rotational Motion of A. The rotational derivative of the E_6 dispersion energy given in eq 13 involves the derivatives of R_{kj} with respect to the rotation of molecule A around the x, y and z axes noted θ_x, θ_y, θ_z. For θ_x, the rotational derivative is given by[24]

$$\frac{\partial R_{jk}}{\partial \theta_{xA}} = \frac{[(y_k - y_j) \cdot (z_k - z_{COM}^A) - (z_k - z_j) \cdot (y_k - y_{COM}^A)]}{R_{kj}}$$

(24)

In eq 24, y_{COM}^A and z_{COM}^A are the y and z coordinates of the center of mass of fragment A, respectively. Similar expressions for $\frac{\partial R_{kj}}{\partial \theta_{yA}}$ and $\frac{\partial R_{kj}}{\partial \theta_{zA}}$ are given in the Supporting Information. The rotational derivatives of the overlap integrals are[24]

$$\frac{\partial S_{kj}}{\partial \theta_{xA}} = \sum_\nu^B c_{\nu j} \sum_\mu^A c_{\mu k} \cdot \sum_a^A \left[\left\langle \frac{\partial \psi_\mu}{\partial z_a} \Big| \psi_\nu \right\rangle \cdot (y_a - y_{COM}^A) \right.$$

$$\left. - \left\langle \frac{\partial \psi_\mu}{\partial y_a} \Big| \psi_\nu \right\rangle \cdot (z_a - z_{COM}^A) \right] + \sum_\nu^B c_{\nu j} \sum_\mu^A \sum_a^A \left(\frac{\partial c_{\mu k}}{\partial \theta_{xA}} \right) \cdot S_{\mu\nu}$$

(25)

As before, the subscripts μ and ν label atomic orbitals, while the subscripts k and j label the localized molecular orbitals. a represents the atoms in fragment A and ψ represents the atomic basis functions. The rotational derivatives of the LMO coefficients c are given in ref.[24] Similar expressions can be obtained for $\frac{\partial S_{kj}}{\partial \theta_{yA}}$ and $\frac{\partial S_{kj}}{\partial \theta_{zA}}$. The rotational derivatives of E_6 can be obtained by substituting eq 24 and eq 25 in eq 13 and eq 14.

In order to obtain the rotational derivatives of $E_{7,0}$, one needs the rotational derivatives of the second and third order T tensors as well as the rotational derivatives of the dynamic dipole–dipole and dipole–quadrupole polarizabilities. The rotation of fragment A around its center of mass can be expressed in terms of the rotation of all of the LMOs of A. The rotation of the electrostatic tensor around the x axis can be expressed as a function of translations in the y–z plane. The rotational derivatives of the electrostatic tensors T are then related to the translational derivatives. For the rotation of the second and third order electrostatic tensors involving LMOs k in fragment A and j in fragment B:

$$\frac{\partial T_{\alpha\beta}^{kj}}{\partial \theta_{xA}} = \frac{\partial T_{\alpha\beta}^{kj}}{\partial y_A} \cdot (z_k - z_{COM}^A) - \frac{\partial T_{\alpha\beta}^{kj}}{\partial z_A} \cdot (y_k - y_{COM}^A)$$

(26)

$$\frac{\partial T_{\gamma\sigma\kappa}^{kj}}{\partial \theta_{xA}} = \frac{\partial T_{\gamma\sigma\kappa}^{kj}}{\partial y_A} \cdot (z_k - z_{COM}^A) - \frac{\partial T_{\gamma\sigma\kappa}^{kj}}{\partial z_A} \cdot (y_k - y_{COM}^A)$$

(27)

Similar expressions can be obtained to describe the rotation of the tensor around the y and z axes (cf., Supporting Information).

The rotational derivatives of the polarizability tensors are obtained by taking the limits of the differences between the rotated tensors and the original tensor in Cartesian coordinates.[26] For the dynamic dipole–dipole polarizabilities of fragment A (LMO superscripts omitted):[26]

$$\frac{\partial \alpha}{\partial \theta_{xA}} = \begin{pmatrix} 0 & \alpha_{xz} & -\alpha_{xy} \\ \alpha_{zx} & \alpha_{yz} + \alpha_{zy} & \alpha_{zz} - \alpha_{yy} \\ -\alpha_{yx} & \alpha_{zz} - \alpha_{yy} & -\alpha_{zy} - \alpha_{yz} \end{pmatrix}$$

(28)

$$\frac{\partial \alpha}{\partial \theta_{yA}} = \begin{pmatrix} -\alpha_{xz} - \alpha_{zx} & -\alpha_{zy} & \alpha_{xx} - \alpha_{zz} \\ -\alpha_{yz} & 0 & \alpha_{yx} \\ \alpha_{xx} - \alpha_{zz} & \alpha_{xy} & \alpha_{zx} + \alpha_{xz} \end{pmatrix}$$

(29)

$$\frac{\partial \alpha}{\partial \theta_{zA}} = \begin{pmatrix} \alpha_{xy} + \alpha_{yx} & \alpha_{yy} - \alpha_{xx} & \alpha_{yz} \\ \alpha_{yy} - \alpha_{xx} & -\alpha_{xy} - \alpha_{yx} & -\alpha_{xz} \\ \alpha_{zy} & -\alpha_{zx} & 0 \end{pmatrix}$$

(30)

A more detailed derivation is given in the Supporting Information along with the derivatives of the dipole–quadrupole polarizability tensor which are obtained in a similar way. The derivative of f^7 given in eq 17 only necessitates the rotational derivatives of the overlap given in eq 25 and in the Supporting Information.

The total torques must also be zero, so that[24,26,36]

$$\tau_{\theta x}^{B(A)} = -\tau_{\theta x}^{A(B)} - [F_y^{A(B)} \cdot (z_{COM}^A - z_{COM}^B) - F_z^{A(B)} \cdot (y_{COM}^A - y_{COM}^B)]$$

$$\tau_{\theta y}^{B(A)} = -\tau_{\theta y}^{A(B)} - [F_z^{A(B)} \cdot (x_{COM}^A - x_{COM}^B) - F_x^{A(B)} \cdot (z_{COM}^A - z_{COM}^B)]$$

$$\tau_{\theta z}^{B(A)} = -\tau_{\theta z}^{A(B)} - [F_x^{A(B)} \cdot (y_{COM}^A - y_{COM}^B) - F_y^{A(B)} \cdot (x_{COM}^A - x_{COM}^B)]$$

(31)

In eq 31, $\tau_{\theta x}^{B(A)}$ represents the x component of the torque on fragment B about the center of mass of B applied by fragment A. $\tau_{\theta x}^{A(B)}$ represents the x component of the torque on fragment A about the center of mass of A exerted by fragment B (the x component of the rotational derivative of the total dispersion energy). $F_x^{A(B)}$ is the x component of the force applied by B on the center of mass of A. $x_{COM}^A - x_{COM}^B$ represents the x component of the distance between the centers of mass of fragment A and fragment B. Similar definitions are given for the y and z components. The rotational derivatives only need to be calculated for one fragment in each fragment pair. The torques for the other fragment can be evaluated using eq 31.

Switching Function. Periodic boundary conditions using the minimum image convention[41] have been implemented for EFP and the distance between the centers of mass is chosen as the distance between molecules.[42] The implementation of a switching function allows the interaction between two fragments to smoothly go to zero as the distance between them increases inside a box, thereby conserving energy during molecular dynamics (MD) simulations.[43] The switching function can be chosen, for example, as a fifth order polynomial.[26] The dispersion interaction energy between two fragments E_{Disp} is scaled by the switching function S:[26]

$$E_S = E_{Disp} S$$

(32)

The derivative of the energy E_S with respect to the translation of fragment A is given by[26]

$$\frac{\partial E_S}{\partial x_A} = E_{Disp} \frac{\partial S}{\partial x_A} + \frac{\partial E_{Disp}}{\partial x_A} S$$

(33)

Similar expressions can be derived for the y and z components. Since the rotational derivatives of the switching function are zero, the rotational derivative of E_S with respect to the rotation of A around the x axis is given by[26]

$$\frac{\partial E_S}{\partial \theta_{xA}} = \frac{\partial E_{Disp}}{\partial \theta_{xA}} S$$

(34)

Again, similar expressions can be derived for the rotational derivative around the y and z axes.

COMPUTATIONAL DETAILS

All calculations have been performed with the quantum chemistry software GAMESS.[21,22] All EFP2 potentials were generated at the RHF/6-311++G(2df,2p) level of theory. The gradient implementation was tested for the parallel displaced benzene dimer,[44] the water trimer,[45] and the ethene-ethyne complex (Figure 1).[44] For all three systems, the analytic and numerical gradients were compared. The systems in Figure 1 were reoptimized using the EFP2 method (labeled structure 1) and at the MP2/6-311++G(2df,2p) level of theory. The quadratic approximation was used for the optimization[46] and the gradient convergence was set to 0.0001 Hartree/Bohr. Another optimization was performed without the E_7 contribution to the dispersion energy (labeled structure 2). The two structures were compared for all 3 systems as well as the E_6 and E_7 contributions to the EFP energy. The water trimer is discussed below and the benzene dimer and ethene-ethyne complex are discussed in the Supporting Information. A molecular dynamics (MD) simulation was performed for a system of 64 water molecules in the NVE ensemble. This simulation was performed on 4 Intel x5460 CPUs (3.16 GHz). Periodic boundary conditions (PBC) were enforced. The MD integrations of translations and rotations of the fragments were performed using the velocity and quaternion Verlet algorithm.[47,48] The MD time step was set to 0.1 fs. The length of the box was set to 12.42 Å, in order to obtain a density of 1000 kg/m³. The distance cutoffs for the switching function were set to r_a = 4.97 Å and r_b = 6.21 Å.

RESULTS AND DISCUSSION

Comparison between Analytic and Numerical Gradients. The analytic and numerical gradients are compared in Table 1 for $[H_2O]_3$, the benzene dimer, and the ethene–ethyne complex (Figure 1). The forces and torques shown in Table 1 correspond to those exerted on one molecule in the system. They are calculated using the EFP2 method, which includes the electrostatic, exchange repulsion, polarization, charge transfer and dispersion energies. The numerical and analytic gradients are in excellent agreement with each other, with errors smaller than 10^{-7} Hartree/Bohr.

Optimization of the Water Trimer. The geometric parameters of structure 1 (optimized with the E_7 contribution to the EFP dispersion energy included), structure 2 (optimized without the E_7 contribution to the EFP dispersion energy), the MP2/6-311++G(2df,2p) optimized trimer, and the structure optimized at the RHF/6-31G(d,p) level of theory[45] are compared in Table 2. The RHF/6-31G(d,p) optimized trimer and atom labels are shown in Figure 2. Overall, the structures
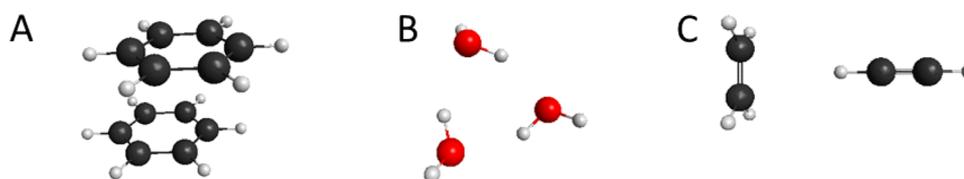
Figure 1. (A) Benzene dimer, (B) H_2O trimer, and (C) ethene−ethyne complex.

Table 1. Comparison of the Analytic and Numerical Gradients in Hartree/Bohr of the Benzene Dimer, Water Trimer and Ethene−Ethyne Complex

system	gradient method	forces			torques		
		x	y	z	θ_x	θ_y	θ_z
$[C_6H_6]_2$	analytic	0.0116568	0.0070467	0.0000083	0.0000047	−0.0000298	0.0181966
	numerical	0.0116568	0.0070467	0.0000083	0.0000047	−0.0000298	0.0181967
$[H_2O]_3$	analytic	−0.0001583	0.0015390	0.0010996	−0.0024685	−0.0003729	−0.0006280
	numerical	−0.0001583	0.0015390	0.0010996	−0.0024684	−0.0003729	−0.0006281
$[C_2H_4]−[C_2H_2]$	analytic	0.0218447	−0.0347514	0.0576795	−0.0000232	0.0001384	0.0001074
	numerical	0.0218447	−0.0347514	0.0576795	−0.0000232	0.0001384	0.0001074

Table 2. Geometrical Structures for the Water Trimer System Optimized at Different Levels of Theory

	structure 1	structure 2	RHF/6-31G(d,p)	MP2/6-311++G(2df,2p)
O1−O4 distance (Å)	2.82	2.78	2.87	2.80
O4−O7 distance (Å)	2.80	2.75	2.88	2.81
O1−O7 distance (Å)	2.81	2.78	2.87	2.81
O1−O4−O7 angle (deg)	60.08	60.12	59.94	59.98
O1−O7−O4 angle (deg)	60.41	60.29	59.77	59.88
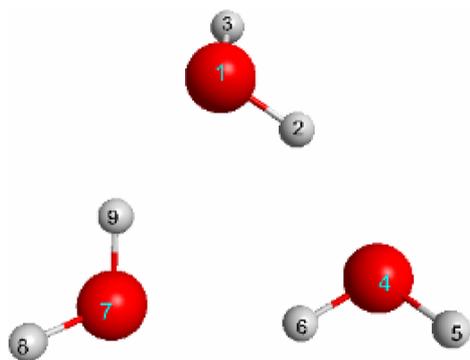
Figure 2. Water trimer optimized at the RHF/6-31G(d,p) level.

Table 3. EFP2 Energy Contributions (in kcal/mol) for the Water Trimer Optimized with and without the E_7 Contribution[a]

	structure 1	structure 2
electrostatic energy (kcal/mol)	−25.73 (45%)	−27.29 (45%)
exchange−repulsion energy (kcal/mol)	18.49 (33%)	21.03 (35%)
polarization energy (kcal/mol)	−5.17 (9%)	−5.71 (9%)
E_6 dispersion energy (kcal/mol)	−3.42 (6%)	−3.69(6%)
E_7 dispersion energy (kcal/mol)	1.10 (2%)	N/A
E_8 dispersion energy (kcal/mol)	−1.14 (2%)	−1.23 (2%)
charge transfer energy (kcal/mol)	−1.64 (3%)	−1.80 (3%)
total EFP energy	−17.52	−18.68
sum of the absolute values of each energy contribution to the total EFP energy (eq 35)	54.50	60.74

[a]The values in parentheses are the percentage contributions of each term to the total EFP interaction energy, as calculated in eq 36 for the electrostatic energy.

obtained at the different levels of theory are very similar, and only one of them is shown in Figure 2. The distance between oxygen atoms is increased by 0.03−0.05 Å when E_7 is included in the dispersion energy. The angles between the three oxygen atoms are very similar as well. Structure 1 is more similar to the MP2 optimized structure than structure 2, which does not include E_7. In order to determine the percentage of each energy contribution to the total energy, the sum of the absolute values of each contribution is calculated in the following manner:

$$\text{sum} = |\text{electrostatic}| + |\text{exchange repulsion}|$$
$$+ |\text{polarization}| + |E_6| + |E_7| + |E_8| + |\text{charge transfer}| \quad (35)$$

The calculated values of "sum" for structures 1 and 2 are given in Table 3. The percentage of the electrostatic energy contribution is then given by

$$|\text{electrostatic}|/(|\text{electrostatic}| + |\text{exchange repulsion}|$$
$$+ |\text{polarization}| + |E_6| + |E_7| + |E_8| + |\text{charge transfer}|) \times 100 \quad (36)$$

The other energy contributions are calculated in a similar manner and given in Table 3.

The percentage contribution of the dispersion energy to the total EFP energy given by

$$(|E_6| + |E_7| + |E_8|)/(|\text{electrostatic}| + |\text{exchange repulsion}|$$
$$+ |\text{polarization}| + |E_6| + |E_7| + |E_8| + |\text{charge transfer}|) \times 100$$

Calculated in this way, the dispersion energy represents 10% of the total EFP energy. The E_7 term only represents
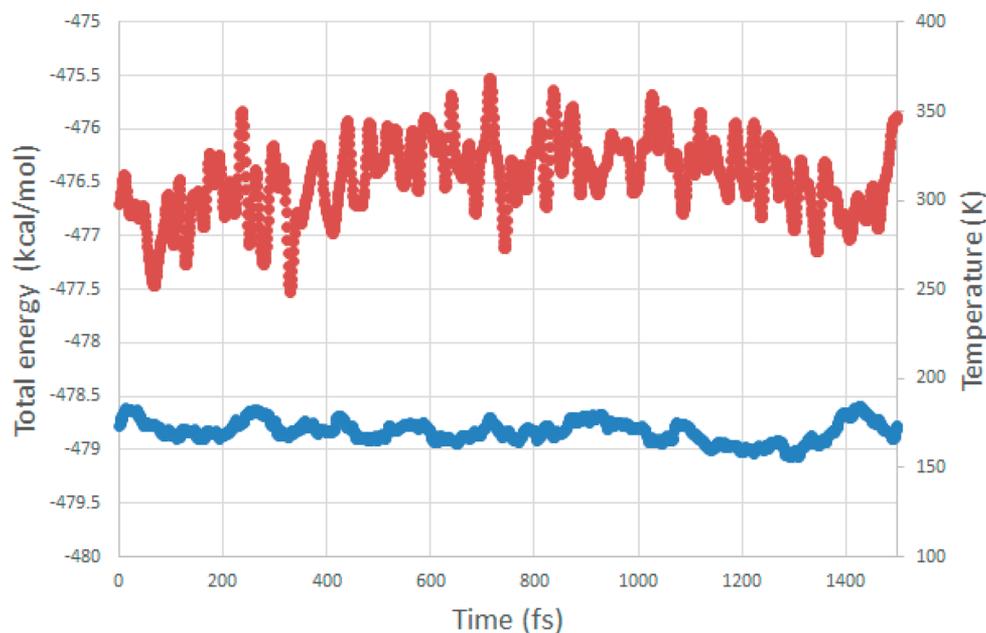
Figure 3. Total energy (in blue) and temperature (in red) of $(H_2O)_{64}$ as a function of the simulation time.

2% of the EFP energy. The contribution of E_7 to the dispersion energy is computed with the formula: $\frac{|E_7|}{|E_6| + |E_7| + |E_8|} \times 100$

Calculated in this way, the E_7 dispersion term represents 20% of the dispersion energy, which is not negligible. Note that E_7, unlike E_6, can be either positive or negative. It can also be zero. For instance, the E_7 energy for the H_2 dimer is zero since the dynamic dipole−quadrupole polarizability of H_2 is zero (the inversion center of H_2 is the same as the inversion center of the LMO).[18] Therefore, it is not just a simple matter of scaling to account for the E_7 contribution to the dispersion energy.

The ethyne-ethene complex and benzene dimer were also optimized in a similar fashion and are discussed in the supporting material. Overall, inclusion of the E_7 dispersion energy leads to geometries more similar to MP2 than when E_7 is not included.

Molecular Dynamics Simulation of 64 Water Molecules in the *NVE* Ensemble. The $(H_2O)_{64}$ system was first equilibrated for 10 000 steps, followed by a production run of 15,000 steps. The total EFP energy (including electrostatics, polarization, exchange−repulsion, charge transfer and dispersion) is considered. The overlap-based damping correction is used for the screening of the electrostatic interaction and a Gaussian formula is used for the polarization screening.[49] The total energy and temperature of the 64-water molecules is plotted as a function of time in Figure 3. Overall, the energy is well conserved, fluctuating by 0.24 kcal/mol from the average value of −478.83 kcal/mol. The temperature deviates by up to about 64 K from the average of 313 K. The E_7/E_6 ratio is 0.16, which is not negligible.

CONCLUSIONS

The analytic gradients of the $E_7(R^{-7})$ term of the dispersion energy, including the overlap-based damping function, were derived and implemented in GAMESS. The expression for the analytic derivative was tested on a few systems by comparing the analytic and numerical gradients, which are in excellent agreement with each other. A geometry optimization was performed on a water trimer. The E_7 term slightly affects the

optimized geometry as shown by the increased intermolecular distances. The E_7 term represents 2% of the EFP energy and 20% of the dispersion energy, which is not negligible. An MD simulation was performed on 64 water molecules with periodic boundary conditions in the *NVE* ensemble and the energy is well conserved. The current implementation of the gradient of the E_7 dispersion term will allow more accurate geometries during optimizations and MD simulations as well as more accurate dispersion energies at a low additional computational cost. This will be particularly useful for modeling slow-moving systems such as proteins. While the implementation of the E_7 contributions to the interaction energy and energy gradient have been assessed using the EFP method, the implications regarding the importance of the E_7 term for intermolecular interactions are general: The R^{-7} contribution to the dispersion interaction energy should not be ignored.

ASSOCIATED CONTENT

ⓢ Supporting Information

The Supporting Information is available free of charge on the ACS Publications website at DOI: 10.1021/acs.jpca.5b11042.

Mathematical calculations and optimization of the ethene−ethyne complex and the benzene dimer (PDF)

AUTHOR INFORMATION

Corresponding Author

*E-mail: mark@si.msg.chem.iastate.edu. Telephone: 515-294-0452.

Notes

ACKNOWLEDGMENTS

REFERENCES

(1) Stone, A. *The Theory of Intermolecular Forces*; 2nd ed.; Oxford University Press: Oxford, 2013.

(2) London, F. The General Theory of Molecular Forces. *Trans. Faraday Soc.* **1937**, *33*, 8b−26.

(3) Grimme, S.; Antony, J.; Ehrlich, S.; Krieg, H. A Consistent and Accurate Ab Initio Parametrization of Density Functional Dispersion Correction (DFT-D) for the 94 Elements H-Pu. *J. Chem. Phys.* **2010**, *132*, 154104.

(4) Grimme, S. Semiempirical GGA-Type Density Functional Constructed with a Long-Range Dispersion Correction. *J. Comput. Chem.* **2006**, *27*, 1787−1799.

(5) Grimme, S. Accurate Description of Van Der Waals Complexes by Density Functional Theory Including Empirical Corrections. *J. Comput. Chem.* **2004**, *25*, 1463−1473.

(6) Schröder, H.; Creon, A.; Schwabe, T. Reformulation of the D3(Becke−Johnson) Dispersion Correction without Resorting to Higher Than C_6 Dispersion Coefficients. *J. Chem. Theory Comput.* **2015**, *11*, 3163−3170.

(7) Kronik, L.; Tkatchenko, A. Understanding Molecular Crystals with Dispersion-Inclusive Density Functional Theory: Pairwise Corrections and Beyond. *Acc. Chem. Res.* **2014**, *47*, 3208−3216.

(8) Tkatchenko, A.; Scheffler, M. Accurate Molecular Van Der Waals Interactions from Ground-State Electron Density and Free-Atom Reference Data. *Phys. Rev. Lett.* **2009**, *102*, 073005.

(9) Tkatchenko, A.; Ambrosetti, A.; DiStasio, R. A. Interatomic Methods for the Dispersion Energy Derived from the Adiabatic Connection Fluctuation-Dissipation Theorem. *J. Chem. Phys.* **2013**, *138*, 074106.

(10) Johnson, E. R.; Becke, A. D. A Post-Hartree−Fock Model of Intermolecular Interactions. *J. Chem. Phys.* **2005**, *123*, 024101.

(11) Amovilli, C.; Floris, F. M. Study of Dispersion Forces with Quantum Monte Carlo: Toward a Continuum Model for Solvation. *J. Phys. Chem. A* **2015**, *119*, 5327−5334.

(12) Pomogaeva, A.; Chipman, D. M. New Implicit Solvation Models for Dispersion and Exchange Energies. *J. Phys. Chem. A* **2013**, *117*, 5812−5820.

(13) Pomogaeva, A.; Chipman, D. M. Hydration Energy from a Composite Method for Implicit Representation of Solvent. *J. Chem. Theory Comput.* **2014**, *10*, 211−219.

(14) Marenich, A. V.; Cramer, C. J.; Truhlar, D. G. Uniform Treatment of Solute−Solvent Dispersion in the Ground and Excited Electronic States of the Solute Based on a Solvation Model with State-Specific Polarizability. *J. Chem. Theory Comput.* **2013**, *9*, 3649−3659.

(15) Duignan, T. T.; Parsons, D. F.; Ninham, B. W. A Continuum Solvent Model of the Multipolar Dispersion Solvation Energy. *J. Phys. Chem. B* **2013**, *117*, 9412−9420.

(16) Duignan, T. T.; Parsons, D. F.; Ninham, B. W. A Continuum Model of Solvation Energies Including Electrostatic, Dispersion, and Cavity Contributions. *J. Phys. Chem. B* **2013**, *117*, 9421−9429.

(17) Adamovic, I.; Gordon, M. S. Dynamic Polarizability, Dispersion Coefficient C_6 and Dispersion Energy in the Effective Fragment Potential Method. *Mol. Phys.* **2005**, *103*, 379−387.

(18) Xu, P.; Zahariev, F.; Gordon, M. S. The R^{-7} Dispersion Interaction in the General Effective Fragment Potential Method. *J. Chem. Theory Comput.* **2014**, *10*, 1576−1587.

(19) Gordon, M. S.; Mullin, J. M.; Pruitt, S. R.; Roskop, L. B.; Slipchenko, L. V.; Boatz, J. A. Accurate Methods for Large Molecular Systems. *J. Phys. Chem. B* **2009**, *113*, 9646−9663.

(20) Pruitt, S. R.; Steinmann, C.; Jensen, J. H.; Gordon, M. S. Fully Integrated Effective Fragment Molecular Orbital Method. *J. Chem. Theory Comput.* **2013**, *9*, 2235−2249.

(21) Gordon, M. S.; Schmidt, M. W. *Advances in Electronic Structure Theory: Gamess a Decade Later*; Elsevier: Amsterdam, 2005.

(22) Schmidt, M. W.; Baldridge, K. K.; Boatz, J. A.; Elbert, S. T.; Gordon, M. S.; Jensen, J. H.; Koseki, S.; Matsunaga, N.; Nguyen, K. A.; Su, S.; et al. General Atomic and Molecular Electronic Structure System. *J. Comput. Chem.* **1993**, *14*, 1347−1363.

(23) Slipchenko, L. V.; Gordon, M. S. Electrostatic Energy in the Effective Fragment Potential Method: Theory and Application to Benzene Dimer. *J. Comput. Chem.* **2007**, *28*, 276−291.

(24) Li, H.; Gordon, M. Gradients of the Exchange-Repulsion Energy in the General Effective Fragment Potential Method. *Theor. Chem. Acc.* **2006**, *115*, 385−390.

(25) Li, H.; Gordon, M. S.; Jensen, J. H. Charge Transfer Interaction in the Effective Fragment Potential Method. *J. Chem. Phys.* **2006**, *124*, 214108.

(26) Li, H.; Netzloff, H. M.; Gordon, M. S. Gradients of the Polarization Energy in the Effective Fragment Potential Method. *J. Chem. Phys.* **2006**, *125*, 194103.

(27) Ghosh, D.; Kosenkov, D.; Vanovschi, V.; Flick, J.; Kaliman, I.; Shao, Y.; Gilbert, A. T. B.; Krylov, A. I.; Slipchenko, L. V. Effective Fragment Potential Method in Q-Chem: A Guide for Users and Developers. *J. Comput. Chem.* **2013**, *34*, 1060−1070.

(28) Turney, J. M.; Simmonett, A. C.; Parrish, R. M.; Hohenstein, E. G.; Evangelista, F. A.; Fermann, J. T.; Mintz, B. J.; Burns, L. A.; Wilke, J. J.; Abrams, M. L.; et al. Psi4: An Open-Source Ab Initio Electronic Structure Program. *Wiley Interdiscip. Rev. Comput. Mol. Sci.* **2012**, *2*, 556−565.

(29) Donchev, A. G. Many-Body Effects of Dispersion Interaction. *J. Chem. Phys.* **2006**, *125*, 074713.

(30) Yu, K.; Schmidt, J. R. Many-Body Effects Are Essential in a Physically Motivated CO_2 Force Field. *J. Chem. Phys.* **2012**, *136*, 034503.

(31) Tkatchenko, A.; DiStasio, R. A.; Car, R.; Scheffler, M. Accurate and Efficient Method for Many-Body Van Der Waals Interactions. *Phys. Rev. Lett.* **2012**, *108*, 236402.

(32) Lao, K. U.; Herbert, J. M. Accurate and Efficient Quantum Chemistry Calculations for Noncovalent Interactions in Many-Body Systems: The XSAPT Family of Methods. *J. Phys. Chem. A* **2015**, *119*, 235−252.

(33) DiStasio, R. A.; von Lilienfeld, O. A.; Tkatchenko, A. Collective Many-Body Van Der Waals Interactions in Molecular Systems. *Proc. Natl. Acad. Sci. U. S. A.* **2012**, *109*, 14791−14795.

(34) McDaniel, J. G.; Schmidt, J. R. First-Principles Many-Body Force Fields from the Gas Phase to Liquid: A "Universal" Approach. *J. Phys. Chem. B* **2014**, *118*, 8042−8053.

(35) Jensen, J.; Gordon, M. An Approximate Formula for the Intermolecular Pauli Repulsion between Closed Shell Molecules. *Mol. Phys.* **1996**, *89*, 1313−1325.

(36) Day, P. N.; Jensen, J. H.; Gordon, M. S.; Webb, S. P.; Stevens, W. J.; Krauss, M.; Garmer, D.; Basch, H.; Cohen, D. An Effective Fragment Method for Modeling Solvent Effects in Quantum Mechanical Calculations. *J. Chem. Phys.* **1996**, *105*, 1968−1986.

(37) Edmiston, C.; Ruedenberg, K. Localized Atomic and Molecular Orbitals. *Rev. Mod. Phys.* **1963**, *35*, 457−464.

(38) Amos, R. D.; Handy, N. C.; Knowles, P. J.; Rice, J. E.; Stone, A. J. Ab-Initio Prediction of Properties of Carbon Dioxide, Ammonia, and Carbon Dioxide···Ammonia. *J. Phys. Chem.* **1985**, *89*, 2186−2192.

(39) Guidez, E. B.; Gordon, M. S. Dispersion Correction Derived from First Principles for Density Functional Theory and Hartree−Fock Theory. *J. Phys. Chem. A* **2015**, *119*, 2161−2168.

(40) Quinet, O.; Liégeois, V.; Champagne, B. Champagne, B. TDHF Evaluation of the Dipole−Quadrupole Polarizability and Its Geometrical Derivatives. *J. Chem. Theory Comput.* **2005**, *1*, 444−452.

(41) Metropolis, N.; Rosenbluth, A. W.; Rosenbluth, M. N.; Teller, A. H.; Teller, E. Equation of State Calculations by Fast Computing Machines. *J. Chem. Phys.* **1953**, *21*, 1087−1092.

(42) Netzloff, H. M.; Gordon, M. S. The Effective Fragment Potential: Small Clusters and Radial Distribution Functions. *J. Chem. Phys.* **2004**, *121*, 2711−2714.

(43) Leach, A. R. *Molecular Modelling: Principles and Applications*; Pearson education: 2001.

(44) Jurečka, P.; Šponer, J.; Černy, J.; Hobza, P. Benchmark Database of Accurate (MP2 and CCSD(T) Complete Basis Set Limit) Interaction Energies of Small Model Complexes, DNA Base Pairs, and Amino Acid Pairs. *Phys. Chem. Chem. Phys.* **2006**, *8*, 1985−1993.

(45) Maheshwary, S.; Patel, N.; Sathyamurthy, N.; Kulkarni, A. D.; Gadre, S. R. Structure and Stability of Water Clusters $(H_2O)_N$, N = 8−20: An Ab Initio Investigation. *J. Phys. Chem. A* **2001**, *105*, 10525−10537.

(46) Culot, P.; Dive, G.; Nguyen, V. H.; Ghuysen, J. M. A Quasi-Newton Algorithm for First-Order Saddle-Point Location. *Theor. Chim. Acta* **1992**, *82*, 189−205.

(47) Swope, W. C.; Andersen, H. C.; Berens, P. H.; Wilson, K. R. A Computer Simulation Method for the Calculation of Equilibrium Constants for the Formation of Physical Clusters of Molecules: Application to Small Water Clusters. *J. Chem. Phys.* **1982**, *76*, 637−649.

(48) Martys, N. S.; Mountain, R. D. Velocity Verlet Algorithm for Dissipative-Particle-Dynamics-Based Models of Suspensions. *Phys. Rev. E: Stat. Phys., Plasmas, Fluids, Relat. Interdiscip. Top.* **1999**, *59*, 3733−3736.

(49) Slipchenko, L. V.; Gordon, M. S. Damping Functions in the Effective Fragment Potential Method. *Mol. Phys.* **2009**, *107*, 999−1016.